Two Crystal Structures of Pneumococcal Pilus Sortase C Provide Novel Insights into Catalysis and Substrate Specificity

ARTICLE *in* JOURNAL OF MOLECULAR BIOLOGY · SEPTEMBER 2009

Impact Factor: 4.33 · DOI: 10.1016/j.jmb.2009.08.058 · Source: PubMed

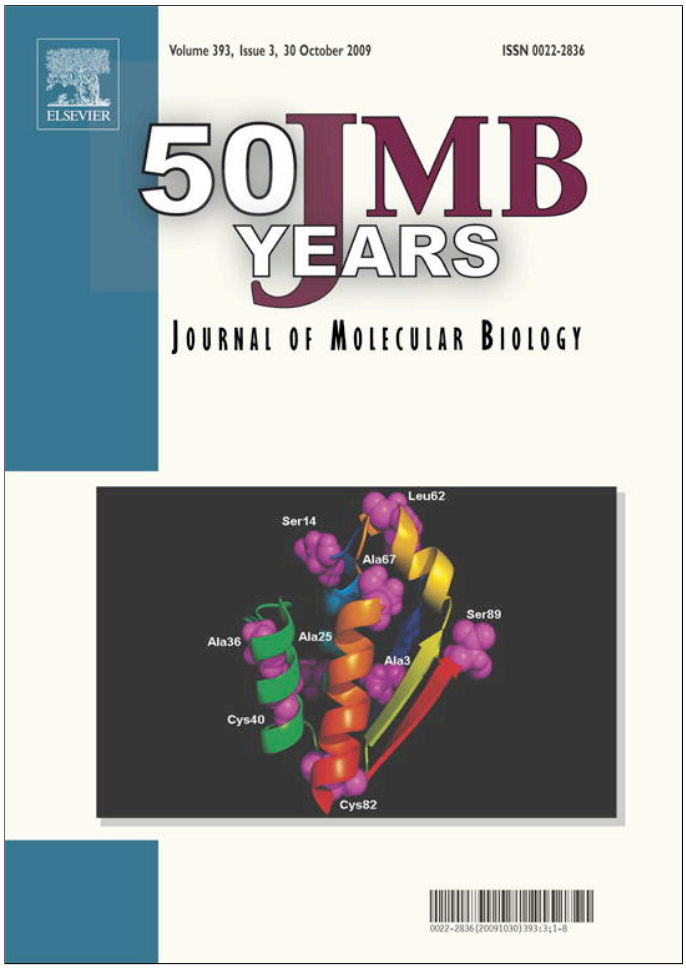

doi:10.1016/j.jmb.2009.08.058 J. Mol. Biol. (2009) 393, 704–716

JMB

Available online at www.sciencedirect.com

ScienceDirect

ELSEVIER

Two Crystal Structures of Pneumococcal Pilus Sortase C Provide Novel Insights into Catalysis and Substrate Specificity

Fabrice Neiers[1,2,3], Chaithanya Madhurantakam[2]†, Stefan Fälker[1,3]†, Clothilde Manzano[4], Andrea Dessen[4], Staffan Normark[1], Birgitta Henriques-Normark[1,3]*‡ and Adnane Achour[2]*‡

[1]*Department of Microbiology, Tumor and Cell Biology, Karolinska Institutet, SE-171 77 Solna, Sweden*

[2]*Center for Infectious Medicine, F59, Department of Medicine Huddinge, Karolinska University Hospital Huddinge, Karolinska Institutet, SE-141 86 Stockholm, Sweden*

[3]*Department of Bacteriology, Swedish Institute for Infectious Disease Control, SE-171 82 Solna, Sweden*

[4]*Institut de Biologie Structurale Jean-Pierre Ebel, UMR 5075 (CEA, CNRS, UJF, PSB), 41 rue Jules Horowitz, F-38027 Grenoble, France*

Received 25 June 2009; received in revised form 24 August 2009; accepted 25 August 2009
Available online 31 August 2009

Edited by R. Huber

The respiratory tract pathogen *Streptococcus pneumoniae* is a primary cause of morbidity and mortality worldwide. Pili enhance initial adhesion as well as the capacity of pneumococci to cause pneumonia and bacteremia. Pilus-associated sortases (SrtB, SrtC, and SrtD) are involved in the biogenesis of pneumococcal pili, composed of repeating units of RrgB that create the stalk to which the RrgA adhesin and the preferential pilus tip subunit RrgC are covalently associated. Using single sortase-expressing strains, we demonstrate that both pilin-polymerizing sortases SrtB and SrtC can covalently link pili to the peptidoglycan cell wall, a property shared with the non-pilus-polymerizing enzyme SrtD and the housekeeping sortase SrtA. Comparative analysis of the crystal structures of *S. pneumoniae* SrtC and SrtB revealed structural differences explaining the incapacity of SrtC, but not of SrtB, to incorporate RrgC into the pilus. Accordingly, site-directed mutagenesis of Thr^{160} in SrtB to an arginine as in SrtC (Arg^{160}) partially converted its substrate specificity into that of SrtC. Solving two crystal structures for SrtC suggests that an opening of a flexible lid and a concomitant cysteine rotation are important for catalysis and the activation of the catalytic cysteine of pilus-associated sortases.

Keywords: sortase; crystal structure; substrate recognition; catalysis; pili

Introduction

The human-specific pathogen *Streptococcus pneumoniae* (pneumococcus) is a primary cause of morbidity and mortality worldwide and represents one of the four major infectious disease killers, together with HIV, malaria, and tuberculosis.[1,2] *S. pneumoniae* is the main cause of respiratory tract infections such as otitis media, sinusitis, and community-acquired pneumonia, and it is also an important pathogen in invasive diseases such as septicemia and meningitis. Invasive pneumococcal disease is preceded by initial colonization of the nasopharynx, but the detailed mechanisms of adhesion are still not well understood.

Most bacterial pathogens have long filamentous structures known as pili or fimbriae extending from their surface. These structures are often involved in the initial adhesion of the bacteria to host cells and

*Corresponding authors. Department of Microbiology, Tumor and Cell Biology, Karolinska Institutet, SE-171 77 Solna, Sweden. E-mail addresses: birgitta.henriques@smi.se; adnane.achour@ki.se.

† C.M. and S.F. contributed equally to this work.

‡ B.H.-N. and A.A. are shared last authors.

tissues, as well as to other bacteria, during colonization. Pilus expression mediates host cell responses that depend on the host receptor being recognized and may also increase the host inflammatory responses.[3,4] Until recently, pili had only been recognized as an attribute of Gram-negative bacteria in which they have been well characterized from the genetic, biochemical, and structural perspectives. During the last few years, some major human Gram-positive bacterial pathogens have also been shown to encode pili, and their biogenesis, structure, and function are now being investigated.[3,5–9]

Multiple-drug resistant *S. pneumoniae* strains have emerged over the last 30 years, requiring rapid development of novel preventive and therapeutic approaches including the development of protein-based vaccines.[10] We have previously demonstrated that globally spreading penicillin nonsusceptible pneumococci belong to clonal lineages that frequently carry pili, encoded by the *rlrA* pathogenicity islet, suggesting that pili contribute to the successful spread of these clones.[11] Pili enhance initial adhesion as well as the subsequent capacity of the bacteria to cause pneumonia and bacteremia.[3] The *rlrA* pilus islet in *S. pneumoniae* encodes three surface proteins, RrgA, RrgB, and RrgC, which form the pneumococcal pilus as well as three pilus-associated sortases, SrtB, SrtC, and SrtD.[3,12,13] The stalk of the pneumococcal pilus is composed of repeating units of RrgB to which RrgA and RrgC are covalently associated. The RrgA protein also occurs associated to the cell wall.[3] RrgC is frequently present at the tip of pili but may also appear along the pilus stalk and in proximity of RrgA.[12] RrgA has been shown to be the major pilus-associated adhesin of pneumococcal pili, but RrgC may also have some binding functions.[13]

In general, sortases can be described as membrane-associated transpeptidases that transfer and covalently link surface proteins to the peptidoglycan cell wall.[14,15] The linkage mechanism is initiated by the cleavage between the threonine and glycine residues of the conserved LPXTG motif (where *X* represents any amino acid) in substrate proteins.[15,16] The C-terminal threonine of the surface protein is concomitantly linked to the sortase catalytic cysteine, after which it is incorporated to the cell wall through the formation of an amide bond between the C-terminal threonine and the stem peptide of the peptidoglycan.[14] In contrast to these so-called housekeeping sortases, pilus-associated sortases covalently link the different subunits of the pilus to each other, resulting in the assembly of mature pili.[5,8,17]

The relative contributions of pneumococcal-associated sortases, SrtB, SrtC, and SrtD, have recently been established.[12] While SrtD did not polymerize any of the Rrg subunits, SrtB and SrtC were redundant in terms of their activity, as both were able to polymerize RrgB in order to form the structural backbone of the pilus as well as link RrgA to this backbone. However, in contrast to SrtB, SrtC cannot incorporate RrgC to the pilus.[12] SrtC also differs from SrtB and SrtD in that the absence of

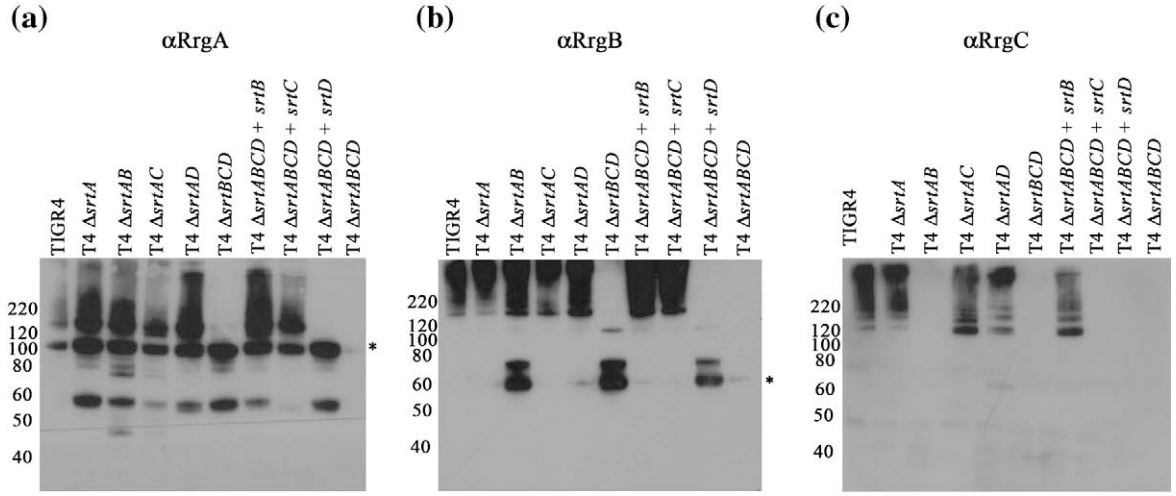

Fig. 1. Role of individual sortases in pilus biogenesis and cell wall anchoring. The production of polymeric high-molecular-mass cell wall-associated pili in isogenic T4 mutants was evaluated by immunoblotting for RrgA (a), RrgB (b), and RrgC (c). In all cases, cell wall proteins were separated by gradient SDS-PAGE, transferred to polyvinylidene fluoride, and probed. Approximate molecular masses are indicated in kilodaltons to the left. The three images show immunoblotting for RrgA (a), RrgB (b), and RrgC (c) in the wild-type TIGR4 ('T4'); the single sortase mutant strain T4Δ*srtA* ('Δ*srtA*'); the double-mutant strains T4Δ*srtAB* ('Δ*srtAB*'), T4Δ*srtAC* ('Δ*srtAC*'), and T4Δ*srtAD* ('Δ*srtAD*'); the triple-mutant strain T4Δ*srtBCD* ('Δ*srtBCD*') that expresses only SrtA; the *trans*-complemented *srtABCD* quadruple-mutant strains T4Δ*srABCD+lacE*::*srtB* ('Δ*srtABCD+srtB*'), T4Δ*srABCD+lacE*::*srtC* ('Δ*srtABCD+srtC*'), and T4Δ*srABCD+lacE*::*srtD* ('Δ*srtABCD+srtD*'); and the quadruple-mutant strain T4Δ*srABCD*. The predicted molecular masses for the RrgA (90 kDa) and RrgB (67 kDa) monomers are indicated by an asterisk. All four sortases are redundant in their capacity to transfer pili and/or pilin monomers to the cell wall. SrtD shows an *in vivo* activity. SrtB and SrtC differ only in their capacity to incorporate RrgC into the pilus.

either of the two latter enzymes, but not of SrtC, abrogates the focal presentation of pilus antigens at the bacterial cell surface.[12]

In the present study, we made use of single sortase-expressing strains to assess the capacity of each of the *S. pneumoniae*-associated sortases (SrtB, SrtC, and SrtD as well as the housekeeping sortase SrtA) to incorporate and link (or not) pilin monomers as well as the polymerized pilus to the peptidoglycan cell wall. We demonstrate that the pilus-polymerizing enzymes SrtB and SrtC can individually covalently anchor pilus polymers to the cell wall, reducing the substrate differences between these two sortases to their capacity to incorporate (SrtB) or not (SrtC) the RrgC pilin subunit into the pilus. Comparing the two crystal structures of the pilus-polymerizing sortase SrtC, solved in this study, with the previously described three-dimensional structure of SrtB,[18] which exhibits different substrate specificities, as well as the nonpolymerizing enzyme (but with pilin cell wall anchoring activity) SrtD provides novel insights into the mechanisms underlying the activation of the catalytic cysteine Cys[221].

Results

All three pilus-associated sortases of *S. pneumoniae* can recognize the peptidoglycan cell wall as substrate for pili and pilin monomers

The first two steps within the proposed model of pilus assembly in Gram-positive organisms consist of the covalent linking of individual pilin subunits followed by the linkage of the polymerized pilus to the peptidoglycan cell wall.[19] It has been demonstrated in *C. diphtheriae* that housekeeping and pilus-associated sortases are able to transfer pili to the cell wall.[20] Furthermore, recent studies also indicated that the capacity of a *S. pneumoniae* strain lacking the housekeeping sortase SrtA to link pili to peptidoglycan is not affected.[21] We have demonstrated that a *S. pneumoniae* strain expressing only SrtA is able to transfer RrgA monomers to the cell wall.[12] Therefore, we hypothesized that at least one of the pilus-associated sortases and the housekeeping SrtA are redundant in their capacity to covalently link pilin proteins to the cell wall peptidoglycan.

In order to address this question and to further determine the specificities of SrtC as compared to SrtA, SrtB, and SrtD, pneumococcal strains lacking diverse combinations of the four sortases were constructed and analyzed for the presence of pili and/or pilus subunits in the cell wall fractions. Our results demonstrate that strains lacking SrtA or lacking a combination of SrtA and any of the pilus-associated sortases still contain pili in the cell wall fractions (Fig. 1). These data indicate that more than one pilus-associated sortase is able to catalyze the transfer of pilin proteins to the peptidoglycan. Surprisingly, even strains that express only one pneumococcal sortase in the genome still display cell wall anchoring activity specific for pilin proteins. Indeed, both SrtB and SrtC transfer pili to the peptidoglycan, while SrtA and SrtD lacking pilus polymerization activity still link RrgA monomers and RrgB monomers (approximately 90 and 67 kDa, respectively, after processing) to the cell wall (Fig. 1). However, linkage of RrgB monomers to the cell wall seems to occur only if no or insufficient RrgB polymerization activity is present. As previously described,[12] an additional band corresponding to a processed RrgA protein with a smaller molecular mass (around 60 kDa) is observed in all strains except for the wild type and the strain without any sortase. This processing event remains to be explained. As also previously described,[12] only SrtB is able to incorporate RrgC in pili (Fig. 1). Furthermore, RrgC monomers are not transferred to the cell wall by any sortase, suggesting that cell surface exposure of this protein is strictly dependent on SrtB-mediated linkage to either RrgA or RrgB. A

Table 1. Data collection and refinement statistics

	SrtC (PDB code 3G66)	SrtC (PDB code 3G69)
Data collection		
Space group	$P2_12_12_1$	$P2_12_12_1$
Cell dimensions		
a, *b*, *c* (Å)	*a*=48.9, *b*=96.9, *c*=98.9	*a*=48.6, *b*=96.5, *c*=98.8
α, β, γ (°)	α=β=γ=90	α=β=γ=90
Observed reflections	350,859 (46,799)	228,540 (28,510)
Unique reflections	52,404 (7580)	31,946 (4490)
Redundancy	6.7 (6.3)	7.2 (6.3)
Completeness (%)	99.8 (99.2)	99.2 (97.2)
R_{merge}[a] (%)	9.3 (51.7)	10.9 (30.5)
$I/\sigma(I)$	14.6 (3.4)	16.1 (6.3)
Refinement		
Resolution (Å)	32.3–1.7 (1.74–1.70)	43.6–2.0 (2.05–2.00)
No. reflections	49,719	30,362
R_{work}/R_{free}[b] (%)	18.7/23.5	19.2/25.8
No. atoms		
Protein	3145	3126
Mes/ion	24	34
Water	557	467
B-factors (Å^2)		
Protein	20.3	23.7
Mes	25.6	24.2
Sulfate ion	—	37.8
Water	40.5	36.2
R.m.s. deviations		
Bond lengths (Å)	0.015	0.023
Bond angles (°)	1.74	2.13
Ramachandran plot (%) (favored, allowed, generous, disallowed)	86.8, 11.1, 2.1, 0	87.2, 10.4, 2.4, 0
PDB code	3G66	3G69

Values in parentheses are for highest-resolution shell.

[a] $R_{merge}=\Sigma_{hkl}\Sigma_i||I_i(hkl)-\{I(hkl)\}||/\Sigma_{hkl}\Sigma_i I_i(hkl)$, where $I_i(hkl)$ is the *i*th observation of reflection *hkl* and {I(*hkl*)} is the weighted average intensity for all observations *i* of reflection *hkl*.

[b] R_{cryst} and $R_{free}=(\sum||F_o|-|F_c||)/(\sum|F_o|)$, where $|F_o|$ is the observed structure-factor amplitude and $|F_C|$ is the calculated structure-factor amplitude. R_{free} is based on 5% of the total reflections excluded from refinement.

quadruple-mutant strain, which does not express any of the pneumococcal sortases, does not contain any pilin protein in the cell wall, demonstrating that covalent linking of pili and/or pilin monomers to the peptidoglycan is strictly sortase dependent and that no other factor/molecule can accomplish this process (Fig. 1). Our mutation study provides the first evidence for an *in vivo* enzymatic role of SrtD in pilus biogenesis in that it is able to covalently link RrgA and RrgB proteins to the peptidoglycan. This enzymatic activity of SrtD probably explains its requirement for regular focal presentation of pilus antigens on the bacterial surface.[12] On the basis of these results, the comparison of the crystal structures of SrtC, SrtB, and SrtD should highlight conserved features characteristic of pilus-specific sortases as well as allow the identification of key residues that dictate differences in substrate specificity.

Overall structure of sortase C

Two crystallization conditions were determined for SrtC.[22] The two crystal structures were solved to 1.7- and 2.0-Å resolutions, respectively (Table 1). The two SrtC structures are identical except for sections of a loop encompassing residues 79–100 that form a lid, as well as for the conformation of the key catalytic residue Cys[221]. The fold of SrtC corresponds

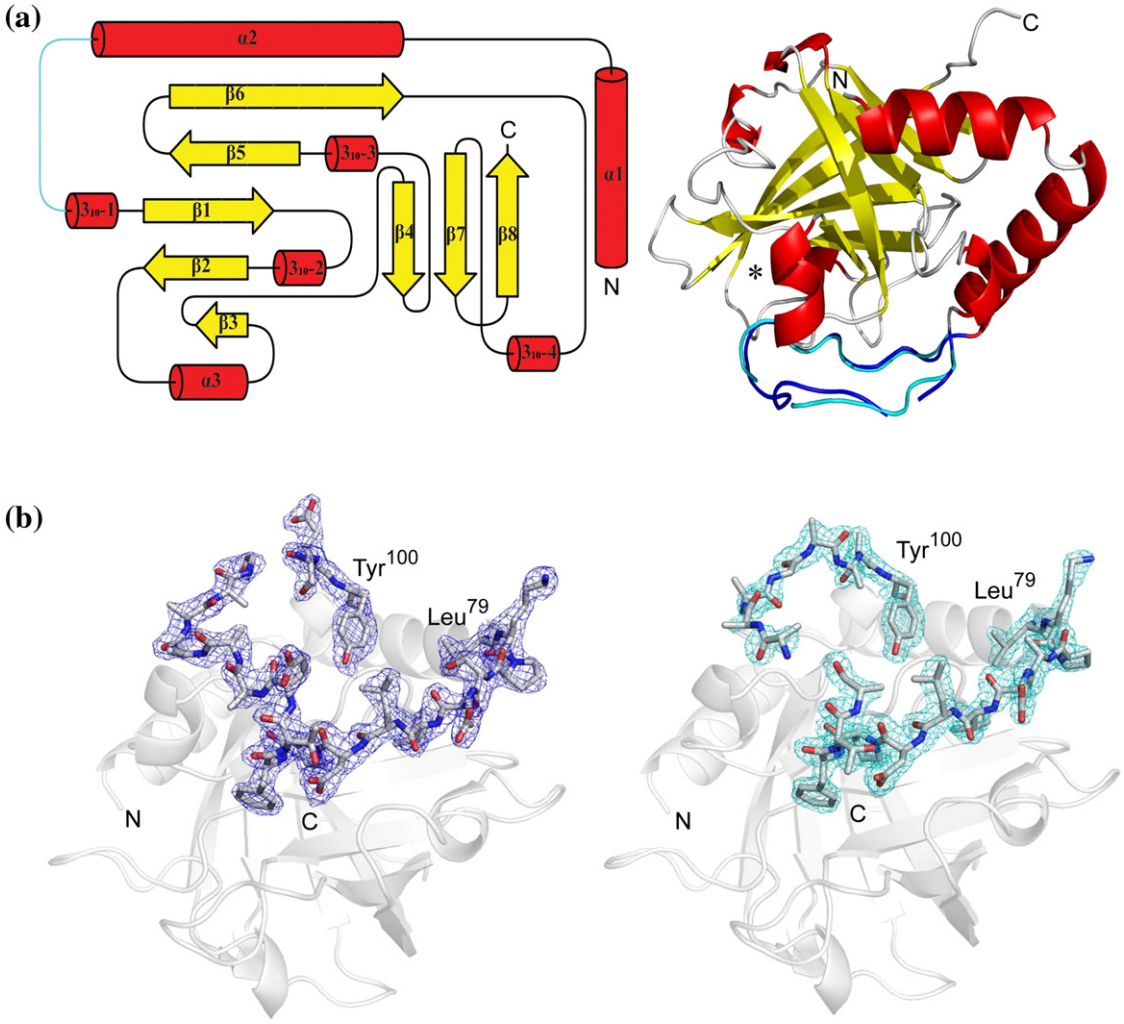

Fig. 2. Topology diagram and overall view of the pilus-associated SrtC from *S. pneumoniae.* (a) The secondary structure diagram of SrtC is displayed to the left with the β-strands in yellow and the 3_{10}- and α-helices in red. The N- and C-termini of the enzyme are indicated by N and C, respectively. The lid specific to pilus-associated sortases is in cyan. The figure was generated using the program TopDraw.[23] An overall view of the crystal structures of the *S. pneumoniae*-derived SrtC is presented to the right. The yellow-colored β-strands form the β-barrel core of the enzyme. Helices are colored in red. The loop consisting of residues 79–100 and that links α2-helix and β1-strand forms a flexible lid that closes the active site, and has different conformations in the two crystal structures of SrtC presented in this study. The loops found in the crystal structures of SrtC (PDB code 3G66) and SrtC (PDB code 3G69) are colored cyan and blue, respectively. The N- and C-termini of the enzyme are indicated by N and C, respectively. (b) The $2F_o - F_c$ electron densities (contoured at 1.0σ) of the lid regions are displayed in blue for SrtC to the left (PDB code 3G69) and in cyan for SrtC (PDB code 3G66) to the right. Residues 79 and 100 are indicated in the figure. Residues 79–100 that correspond to the lid regions of SrtC are shown in stick mode, while the rest of the two structures are colored in transparent white.

to the previously described β-barrel structure, specific for sortases, composed of eight anti-parallel β-strands linked by multiple α- and 3_{10}-helices (Figs. 2a and 3).[24–28] However, in contrast to housekeeping sortases such as SrtA,[24] the structure of SrtC contains a lid that is common to pilus-associated sortases such as SrtB and SrtD in *S. pneumoniae*.[18]

As expected from the sequence identity (58%), the overall fold of SrtC is similar to the recently described crystal structure of SrtB,[18] with an average root mean square deviation (rmsd) upon superposition of all C^{α} atoms for the two structures of 1.2 Å (Fig. 4). Despite lower sequence identity (27%), SrtC also resembles SrtD[18] (with an rmsd of 1.9 Å), although major localized differences can be noted such as the presence of an additional C-terminal helix in SrtD (Figs. 3 and 4). The active site is localized on the external face of the β-barrel and is closed by the lid (Fig. 2a). Although the lid feature is shared by SrtB and SrtD, its conformation is different. The relative mobility is evidenced by the poorer electron density for most of the side chains and some of the main chain of the residues forming the lid (residues 79–85 and 89–100) (Fig. 2b). In contrast, the electron density of the central section of the lid (residues 86–88) that is anchored within the active site through several interactions with key catalytic residues is well defined (Fig. 2a and b). The relatively higher *B*-factor values observed for the lid regions in both crystal structures (41.2 and 45.7 $Å^2$ on average for residues 79–100 in 3G66 and 3G69, respectively) when compared to the overall values (20.3 and 23.7 $Å^2$ on average for 3G66 and 3G69, respectively) argue for a higher mobility of the lid. The quality of the electron density allows a well-defined positioning of most of the main-chain residues of the lid. Thus, the main chain of the lid can adopt at least two different conformations, reflecting further the mobility of the lid (Fig. 2a and b).

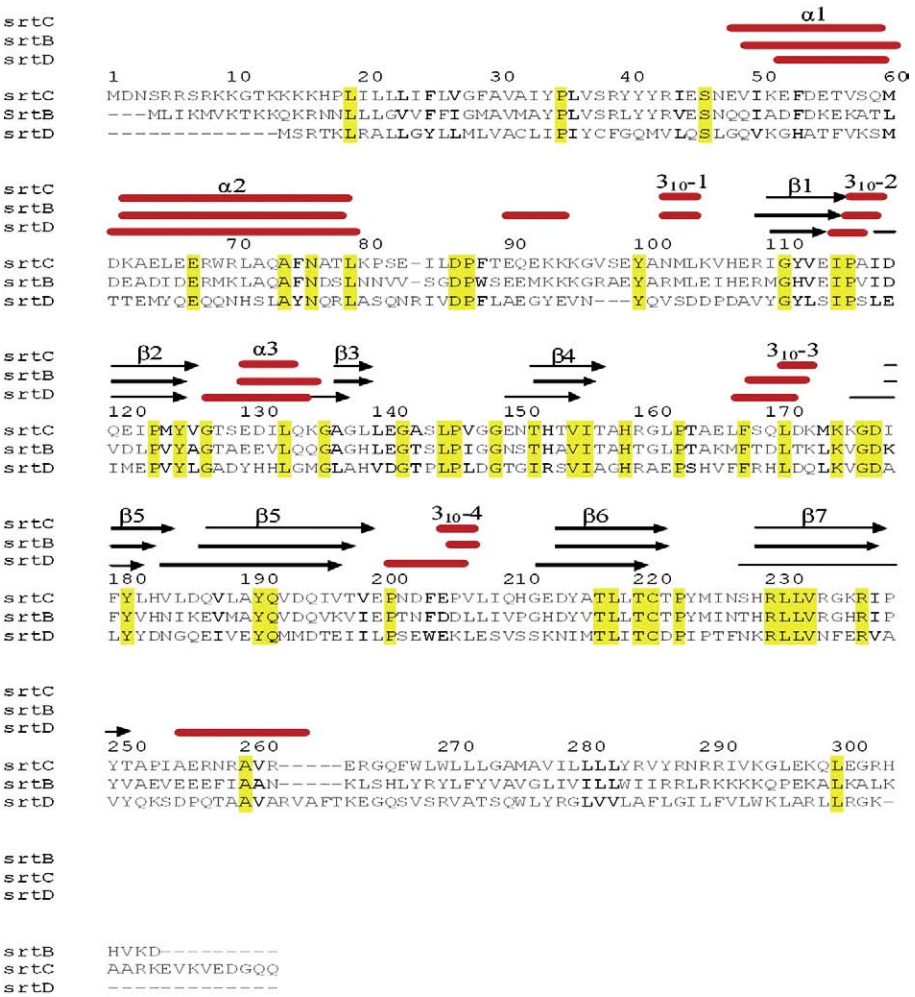

Fig. 3. Sequence alignment of the pilus-associated sortases SrtC, SrtB, and SrtD from *S. pneumoniae*. The numbering used for SrtB and SrtD is aligned on the numbering of the sequence of SrtC. The secondary structures are indicated for each sortase with black arrows (β-strands) and red lines (3_{10}- and α-helices). Identical and similar residues are indicated with black letters on yellow background and black letters only, respectively. The sequences were aligned using the program Bioedit (http://www.mbio.ncsu.edu/BioEdit/bioedit.html).

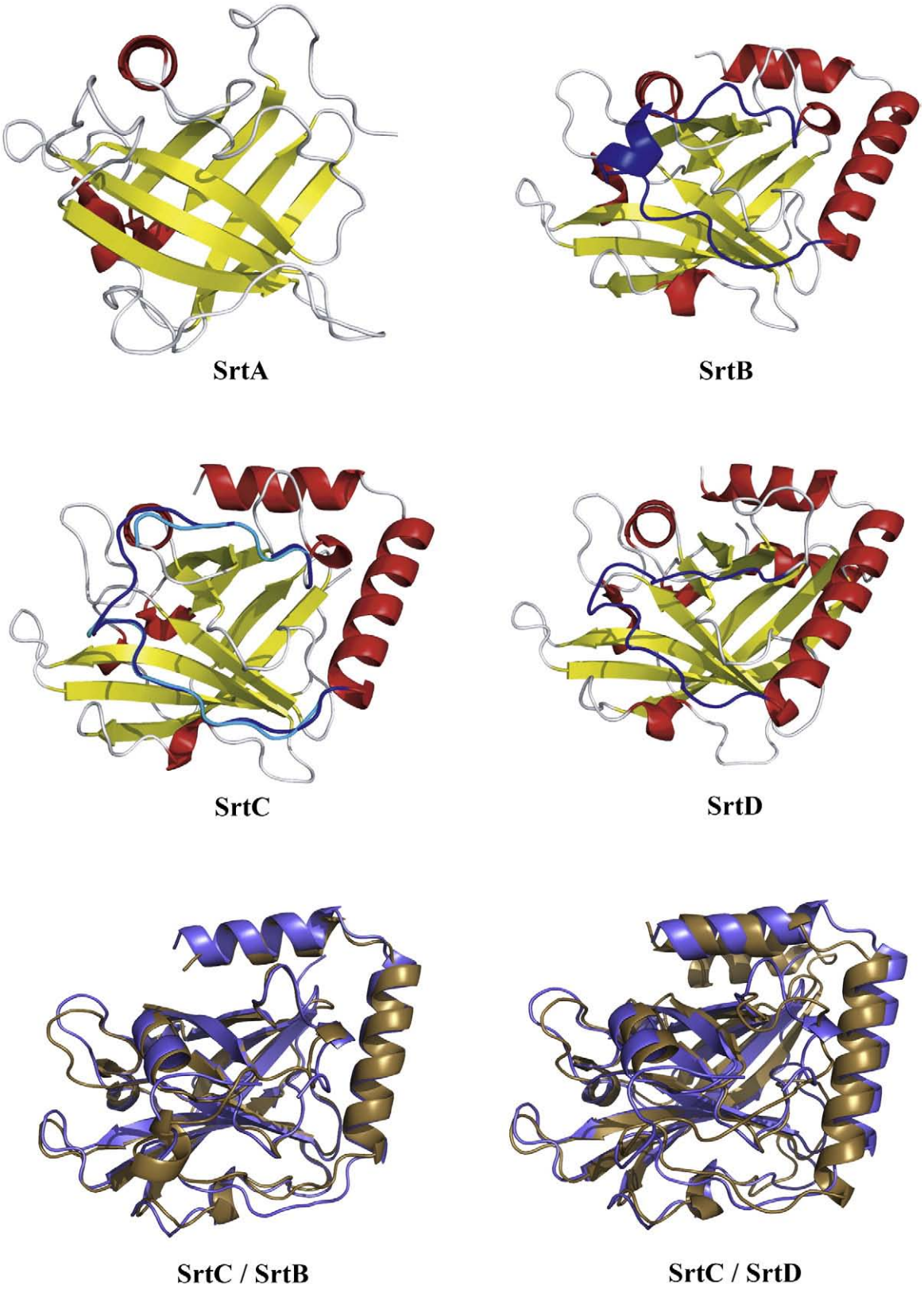

Fig. 4. All pilus-associated sortases from *S. pneumoniae* contain a lid that covers the active site. Structural comparison of the three pilus-associated *S. pneumoniae*-derived sortases, SrtB (PDB code 2W1J), SrtC, and SrtD (PDB code 2W1K), and the housekeeping sortase SrtA derived from *Staphylococcus aureus* (PDB code 1T2P). All three pilus-associated sortases SrtB, SrtC, and SrtD from *S. pneumoniae* display an additional loop (blue) that closes the active site that is absent in the housekeeping sortase SrtA from *S. aureus.* The superpositions of SrtC (purple) with SrtB (gold) and SrtD (gold) are displayed at the bottom of the figure. The structures differ by the lid positioning and an additional helix in the C-terminal region that is only present in SrtD.

The tip of the lid is anchored within the active site through multiple interactions with key catalytic residues

The carboxylate group of the side chain of Asp[86] on the tip of the lid forms a salt bridge with a 'fork-stick' geometry with the side chain of Arg[230] within the active site (Fig. 5).[29] The sulfur atom of the catalytic residue Cys[221] forms a sulfur-aromatic interaction with the aromatic ring of Phe[88], strengthening the anchoring of the lid within the active site.[30] Sulfur-aromatic interactions between cysteine and phenyalanine residues have been described previously as a combination of hydrophobic and electrostatic interactions.[31] Interestingly, sulfur-aromatic interactions are also formed between the catalytic cysteine and a tryptophan or a phenyalanine residue on the lids of SrtB and SrtD, respectively.[18] This indicates a general mechanism for SrtC, SrtB, and SrtD in which a sulfur-aromatic interaction between Cys[221] and an aromatic residue on the lid results in its anchoring within the active site.

Comparative structural analysis suggests a molecular mechanism for catalysis within the active site

It has previously been demonstrated that Cys[221] is essential for the catalytic activity of housekeeping and pilus-associated sortases.[12,32] However, the molecular mechanisms leading to the deprotonation of Cys[221] remain to be defined. The crystal structures of SrtC indicate that the distance between residues His[159] and Cys[221] (>5.1 Å) is not compatible with a direct deprotonation *via* a thiolate–imidazolium pair. Omit map analysis of SrtC (PDB code 3G66) demonstrates that Cys[221] can adopt two different conformations within the active site of

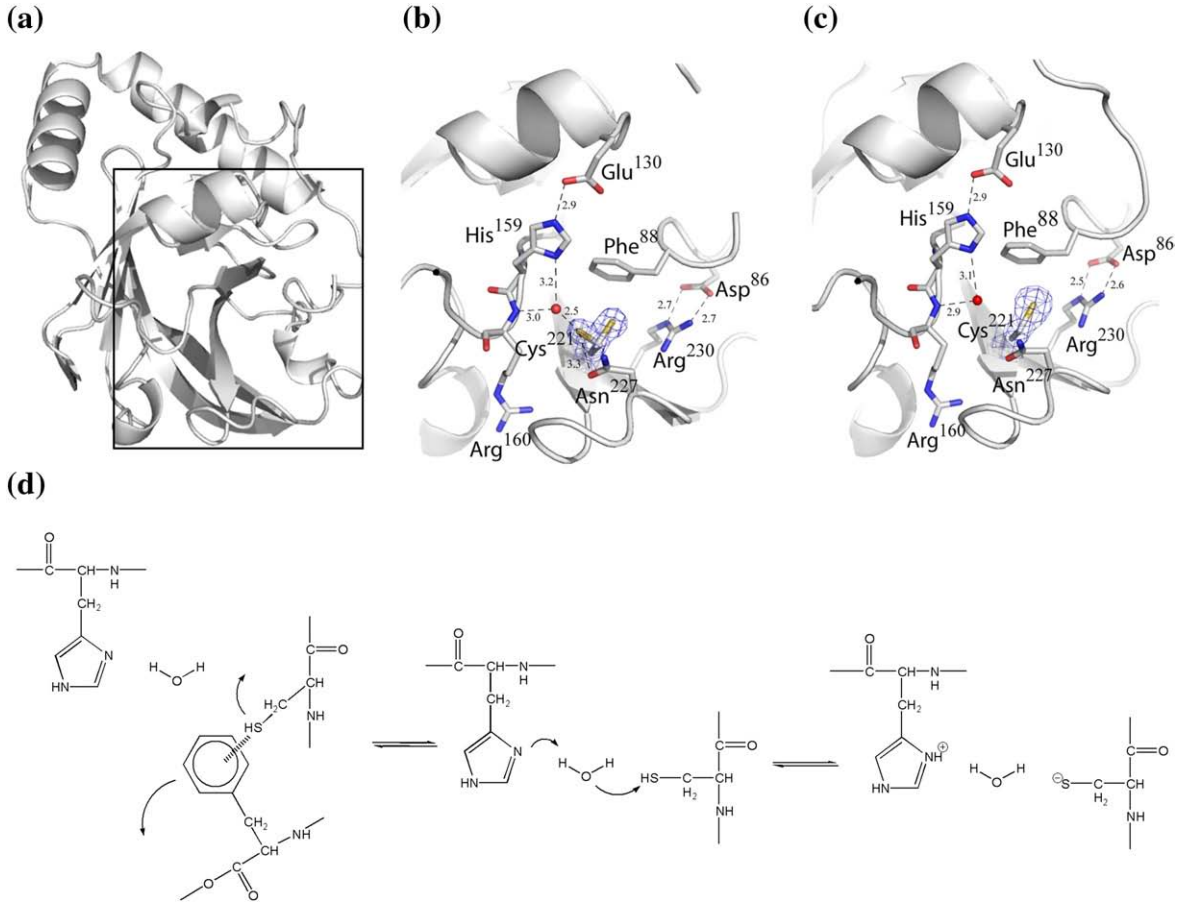

Fig. 5. The catalytic cysteine residue Cys[221] can take two different conformations within the active site of SrtC. (a) An overview of the crystal structure of SrtC; the square indicates the region that is enlarged in (b) and (c). The active sites of SrtC are presented in (b) (PDB code 3G66) and (c) (PDB code 3G69), respectively. While the catalytic cysteine Cys[221] adopts two different conformations (modeled with 0.5 occupancy) in (b), the same residue adopts only one conformation in (c). Electron density (contoured at 1.2 Å) is displayed in blue. Water molecules are indicated by red spheres and hydrogen bonds are shown as broken lines with distances indicated in angstrom. The figure was generated using the program PyMol (Delano Scientific LLC). In (d), a mechanism for the activation of the catalytic cysteine in the pilus-associated sortases is proposed. The substrate binding can be the driving force that disrupts the stabilizing interaction between the catalytic cysteine and the aromatic residue of the loop (Phe for SrtD and SrtC and Trp for SrtB) as observed in the structure display in (c). The cysteine residue becomes available for proton transfer *via* a conserved water molecule (similar to the structure shown in Fig. 4b), resulting in the formation of the active thiolate form.

SrtC (Fig. 5b and c). One conformation of Cys^{221} forms sulfur-aromatic interactions with Phe^{88}, while the second conformation forms a hydrogen bond interaction with a water molecule (WAT^{74}). It should be noted that a water molecule is localized at exactly the same position in the crystal structures of all three described pilus-associated sortases. A network of hydrogen bond interactions is formed within this section of the active site, reaching from Cys^{221} to Glu^{130}. In addition to the hydrogen bond interaction formed with Cys^{221}, WAT^{74} also forms two hydrogen bond interactions with His^{159} and Arg^{160}. In turn, the nitrogen atom N^{ε} of His^{159} forms a hydrogen bond interaction with Glu^{130} (Fig. 5b).

Omit map analysis clearly shows that only one conformation is present for Cys^{221} in the second crystal structure of SrtC (PDB code 3G69) (Fig. 5c). It should be noted that the position of the water molecule WAT^{74} is conserved in both crystal structures of SrtC (Figs. 4c and 5b). Thus, other factors may result in the dual or single conformations of Cys^{221} observed in the two crystal structures of SrtC. The interaction with a substrate could open the lid of SrtC, resulting in the disruption of sulfur-aromatic interactions between Phe^{88} and Cys^{221} and an increased propensity for the second conformation of Cys^{221} to occur. The water molecule WAT^{74} would then be able to transfer the proton from Cys^{221} to His^{159}, which is stabilized and properly oriented through hydrogen bond interactions with Glu^{130}. The interactions with Glu^{130} could thereafter result in an increase of the pK_a of His^{159}, allowing for its protonation (Fig. 5d). Cysteine proteases have been previously described to perform a nucleophilic attack on the carbonyl carbon at the scissile peptide bond of the substrate by the thiolate form of Cys^{221}, resulting in the formation of a thioacyl intermediate. A similar relay between the nucleophilic group and the general base by a water molecule has been proposed before for β-lactamases.[33] As also suggested by studies in housekeeping sortases,[25] the oxyanion formed on the thioacyl intermediate would probably be stabilized by interactions with Arg^{230}, which is conserved in all sortases. The second step of the catalytic mechanism would lead to the release of the cleaved peptide before the attack of the thioacyl intermediate by an amine group (from the side chain of the lysine residue in the case of the pilin motif), resulting in the production of a cross-linked peptide and the regeneration of the enzyme. Future determination of the thioacyl intermediate of pilus-associated sortases should provide a better understanding of this mechanism.

Structural differences between SrtC and SrtB explain the incapacity of SrtC to incorporate RrgC in the pilus

In order to build pili, pilus-associated sortases cut LPXTG-like motifs in Rrg molecules (YPRTG for RrgA, IPQTG for RrgB, and VPDTG for RrgC). The cleaved Rrg molecule is thereafter linked to a pili motif such as YPKN, particularly in the case of RrgB–RrgB linking.[8] Subtle modifications within the active sites of SrtC and SrtB may explain the observed differences in the fine specificity and the recognition of substrates by these two sortases.

While the active site of SrtB is mainly occupied by the lid, surface analysis indicates the presence of an empty pocket that could be used for substrate recognition (Fig. 6a). Importantly, the corresponding pocket is occupied by the side chain of residue

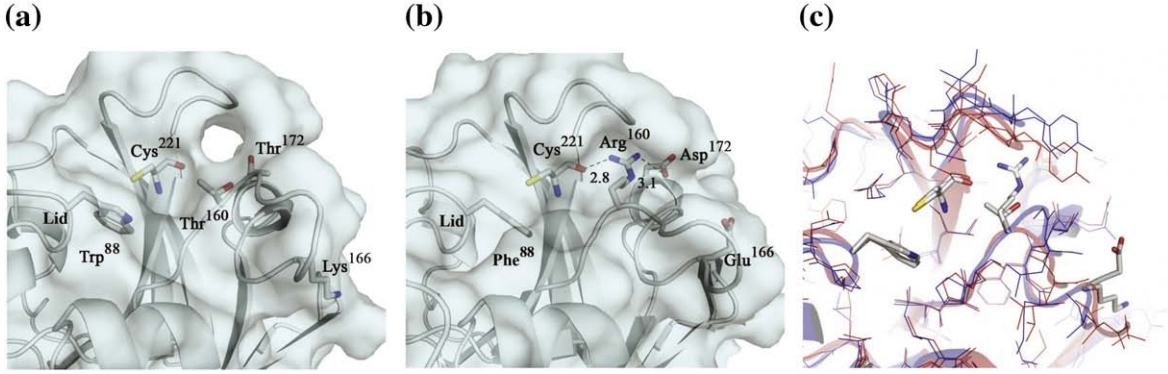

Fig. 6. Comparative structural analysis suggests a molecular explanation for the substrate specificity. Comparison of the active sites of SrtB (PDB code 2W1J) (a) and SrtC (b) provides a structural explanation for the functional differences observed between these two sortases. The side chains of the catalytic cysteines Cys^{221}, as well as the side chains of residues within and near the vicinity of the active site, are displayed. The side chain of the residue Phe^{88} localized on the lid of SrtC, as well as the side chain of the corresponding residue Trp^{60} in SrtB, is displayed. The side chain of residue Arg^{160} in SrtC forms hydrogen bond interactions with the side chain of the Asp^{172} and the oxygen atom of the main chain of Cys^{221}. Hydrogen bonds are shown as black broken lines with distances indicated in angstrom. The side chains of residues Thr^{160} and Thr^{172} in SrtB that correspond to Arg^{160} and Asp^{172} in SrtC, respectively, are smaller, creating a substrate pocket in the active site of SrtB that is not present in SrtC. It should also be noted that the negatively charged residue Glu^{166} present at the surface of SrtC within the vicinity of the active site is substituted to a positively charged lysine residue Lys^{166} in SrtB. A superposition of SrtC (in red) and SrtB (in blue) is provided in (c). As indicated in (a) and (b), the majority of the residues within the active site are conserved (represented in line mode) except for a few residues (represented in stick mode).

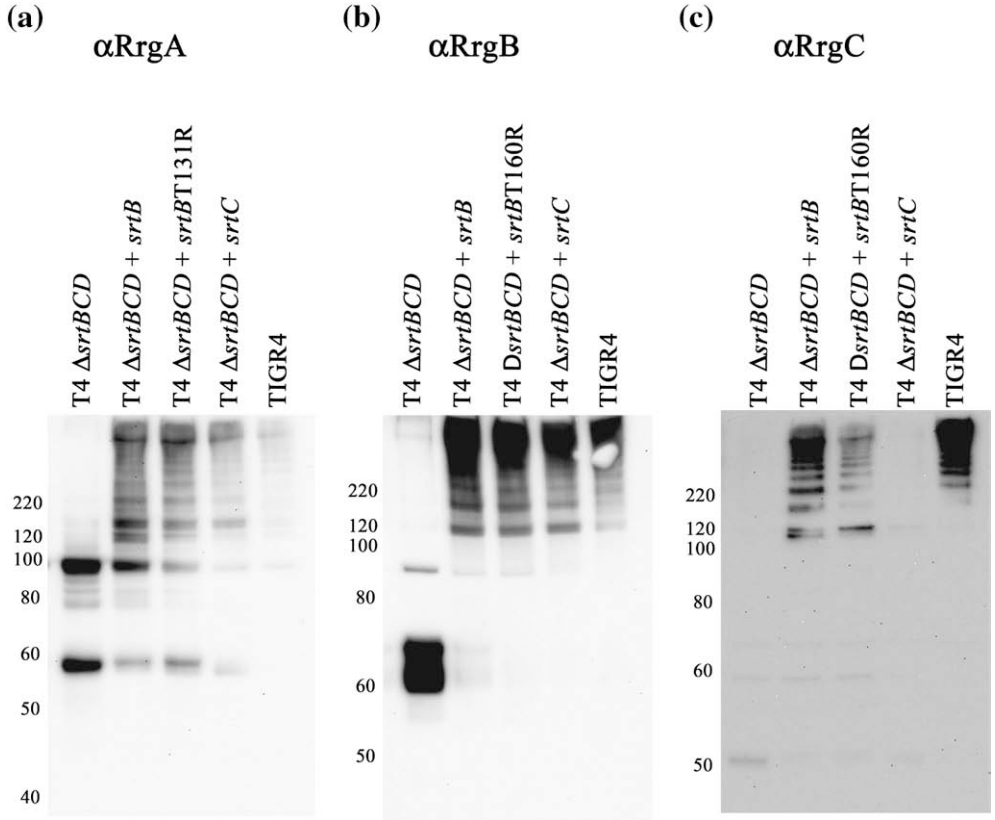

Fig. 7. Substitution of Thr^{160} in SrtB to an arginine (as in SrtC) impairs its capacity to incorporate RrgC. Production of polymeric high-molecular-mass cell wall-associated pili in isogenic T4 mutants was evaluated by immunoblotting for RrgA (a), RrgB (b), and RrgC (c). Approximate molecular masses in kilodaltons are indicated to the left. The three images show immunoblotting for RrgA, RrgB, and RrgC in the triple-mutant strain T4Δ*srtBCD* ('Δ*srtBCD*'), the *trans*-complemented *srtBCD* triple-mutant strain T4Δ*srBCD+lacE*::*srtB* ('Δ*srtBCD+srtB*'), the *srtBCD* triple-mutant strain *trans*-complemented with SrtB with the point mutation Thr^{160}Arg T4Δ*srBCD+lacE*::*srtBT160R* ('Δ*srtBCD+srtB*'T160R), and the *trans*-complemented *srtBCD* triple-mutant strain T4Δ*srBCD+lacE*::*srtC* ('Δ*srtABCD+srtC*'). Substitution of Thr^{160}, one of the few positions in SrtB differing with SrtC, to an arginine as in SrtC affects the capacity of the mutated SrtB to incorporate RrgC.

Arg^{160} in the crystal structures of SrtC (Fig. 6b). The side chain of Arg^{160} in SrtC is stabilized through double hydrogen bond interactions with the main chain of Cys^{221} and the side chain of Asp^{172}. Conversely, the positions corresponding to Arg^{160} and Asp^{172} in SrtC are occupied by two threonines (Thr^{160} and Thr^{172}) in SrtB (Fig. 6a and b). Indeed, repeated *in vivo* analysis of the effects of the substitution of Thr^{160} to an arginine in SrtB clearly reduces its capacity to incorporate RrgC in the pilus, while its capacity to incorporate both RrgA and RrgB remains unaffected (Fig. 7). While the observed effect reveals the importance of Thr^{160} in SrtB, it also indicates that other residues such as Thr^{172} may play a role in the specificity of SrtB in incorporating RrgC (Fig. 6b).

Discussion

The three-dimensional structures of pneumococcal SrtC provide novel information regarding the catalysis and the specificity of this enzyme. The catalytic cysteine of housekeeping sortases such as the *Staphylococcus aureus*-derived SrtA is localized within a hydrophobic pocket,[24] which can probably protect against erroneous oxidation. In contrast, the corresponding catalytic cysteine is hidden by a lid in the pilus-associated SrtB, SrtC, and SrtD, indicating that unregulated oxidation is prevented through an alternative pathway. The two crystal structures of SrtC presented within this study also indicate that the lid is mobile and can take at least two different conformations, suggesting a second important role for the lid in the regulation of substrate accessibility to the active site.[18] The presence of a lid, however, does not strictly correlate to pilin–pilin transpeptidase activity, since SrtD, having a lid, lacks this activity. Furthermore, it is not required for the enzyme to discriminate between peptidoglycan and pilin substrates, since SrtB and SrtC, both having a lid, can use both types of substrates. Also, SrtD, which contains a lid, and SrtA, which most likely lacks a lid in analogy to staphylococcal SrtA, can both use peptidoglycan as substrate for anchoring of pilin. Our structural analysis indicates the dual conformation of the catalytic cysteine in SrtC as an intrinsic general property of pilus-associated

sortases and suggests a general mechanism of catalysis for the pilus-associated sortases described here. Future pK_a determination and *in vitro* kinetic studies should provide a better understanding of this mechanism that is probably similar for all three pilus-associated sortases in pneumococci.

The *in vivo* experiments provided in this study demonstrate the dual functions of SrtC and SrtB comprising pilus building and LPXTG–cell wall anchoring activity. From an evolutionary point of view, our results suggest the existence of a common ancestor for pilus-associated and housekeeping sortases. Since the housekeeping function is conserved among most known Gram-positive bacterial organisms, we hypothesize that the common ancestor was a housekeeping sortase with a β-barrel structure fold. Pilus-associated sortases have most probably evolved from this common ancestor through the addition of structural features such as the lid and an additional α-helix in the case of SrtD.

In this context, it may not be surprising to note that the charge of the solvent-exposed lid is similar when comparing SrtB and SrtC. Both lids possess a positively charged portion composed of three lysine residues (positions 93–95), in contrast to the entire lid in SrtD that is exclusively composed of hydrophobic or negatively charged residues (Fig. 3). The lid could play an important role in the interaction of pilus-associated sortases with substrates, since it can open or close access to the active site. The observed differences in charge on the lid can represent another important aspect that explains why SrtB and SrtC act as pilus-polymerizing enzymes, in contrast to SrtD.

Comparative analysis indicates that very few residues differ between the active sites of SrtB and SrtC. The crystal structures of SrtC reveal that the side chain of residue Arg^{160} in SrtC fills a substrate recognition pocket in the active site. Substitution of the corresponding residue Thr^{160} in SrtB to an arginine demonstrates the essential role of this residue for the incorporation of RrgC. Interestingly, this pocket is also filled in SrtD by an arginine that forms hydrogen bond interactions with the catalytic cysteine and an aspartate residue. This may provide a structural explanation to the fact that SrtD is not able to incorporate RrgC into a pilus polymerized by SrtC. The observed reduction of the *in vivo* capacity of the SrtB mutated variant to incorporate RrgC also indicates that other residues can be involved in the nonrecognition of RrgC by SrtC. Asp^{172}, which stabilizes the positioning of Arg^{160} in SrtC *via* a hydrogen bond interaction, may play an important role for the closing of the recognition pocket in SrtB. Also, if we consider the size of the RrgC protein (30 kDa), the interaction might not be limited to the sortase active site, but other residues involved in surface charge could also determine RrgC recognition. The only difference in surface charge close to the active site is the positively charged Lys^{166} in SrtB replaced by the negatively charged Glu^{166} in SrtC (Fig. 6a and b).

The molecular mechanisms underlying the formation of the pilus still remain to be fully assessed. Our results demonstrate cell wall anchoring activity of SrtB, SrtC, as well as SrtD. Analysis of the two three-dimensional structures of SrtC suggests the mobility of the lid specific to pilus sortases as well as its importance for the activation of the catalytic cysteine residue. *In vivo* experiments demonstrate that the only functional difference between SrtB and SrtC is the incorporation of RrgC in the pilus. The structural comparison of SrtC and SrtB suggested the importance of specific amino acids in the vicinity of the active site for the observed functional differences between these two sortases. Finally, comparison of the two structures of SrtC suggests that rotation of the active-site cysteine close to a water molecule, in association with lid mobility, may allow for deprotonation of the cysteine, resulting in the thiolate form required for forming a thioacyl intermediate with the substrate.

Materials and Methods

Bacterial strains, media, and growth conditions

All the pneumococcal strains used within this study, including isogenic mutant derivatives, are described in Table 2. The insertion–deletion mutagenesis used for most strains as well as the strategy to achieve complementation *in trans* are described elsewhere.[3,35] The primers used for each strain are indicated in Table 2, and all primers are described in Table 3. All resulting strains were checked by PCR, sequencing, and immunogenicity, thereby demonstrating a lack of polar effects of deletion of one subunit gene on the expression of other genes. Unless otherwise noted, bacteria were streaked from frozen stocks onto blood plates with appropriate selection for overnight growth and inoculated briefly into pre-warmed DS (dextrose–serum) medium (OXOID manual, 1990). DS was thereafter inoculated into pre-warmed C + Y medium in order to achieve an absorbance of 0.05 when measured at a wavelength of 620 nm. Cultures were permitted to grow to mid-log ($A_{620} = 0.4$) at 37 °C without agitation before collection for experimentation.

Cell wall preparation and immunoblotting

Cell wall-associated proteins were isolated from genetically defined strains of S. pneumoniae and analyzed as previously described.[3]

Protein expression and purification

DNA encoding residues 46 to 267 of the SrtC protein from *S. pneumoniae* (TIGR4, SP_0467) was cloned into the NdeI and SacI restriction sites of the pET24c plasmid (Novagen). The resulting construct was transformed into *Escherichia coli* BL21 (DE3) pLysS (Novagen) for overexpression at 37 °C. The cultures were maintained at 37 °C for 12 h after induction with isopropyl-D-1-thiogalactopyranoside. SrtC was purified following previously described procedures.[22]

Table 2. Characteristics of strains or mutants used in the study

Strain/mutant	Relevant characteristics	Primers employed in construction	Source/reference
T4	TIGR4 piliated invasive isolate	Not applicable	3
T4Δ*srtA*	Kan^R, strain lacking *srtA*	Upstream: SrtA-1 and SrtA-2; downstream: SrtA-3 and SrtA-4; Kan-resistance cassette from Janus-fragment: Dam406 and Kan-Rev-Apa	34; this study
T4Δ*srtAB*	Erm^R, Kan^R, strain lacking *srtA* and *srtB*	SrtA-1/SrtA-4 fragment moved from T4Δ*srtA* to T4Δ*srtB*	12; this study
T4Δ*srtAC*	Erm^R, Kan^R, strain lacking *srtA* and *srtC*	SrtA-1/SrtA-4 fragment moved from T4Δ*srtA* to T4Δ*srtC*	12; this study
T4Δ*srtAD*	Erm^R, Kan^R, strain lacking *srtA* and *srtD*	SrtA-1/SrtA-4 fragment moved from T4Δ*srtA* to T4Δ*srtD*	12; this study
T4Δ*srtBCD*	Erm^R, strain lacking *srtB, srtC,* and *srtD*, expressing *srtA*	Upstream: SrtB-1 and SrtB-2; downstream: SrtD-3 and SrtD-4	12
T4Δ*srtBCD*+ *lacE*::*srtB*	Spc^R, Erm^R, T4Δ*srtBCD* containing *srtB in trans*	Upstream: NlacEF and SpcR1; coding sequence: SrtB-aad9 and Sp0479-SrtB; downstream: NlacER and Sp0479R	12
T4Δ*srtBCD*+ *lacE*::*srtC*	Spc^R, Erm^R, T4Δ*srtBCD* containing *srtC in trans*	Upstream: NlacEF and SpcR1-EcoRI; coding sequence: SrtC5′-EcoRI and SrtC3′-HindIII; downstream: NlacER and Sp0479R-HindIII	12
T4Δ*srtBCD*+ *lacE*::*srtB*T131R	Spc^R, Erm^R, T4Δ*srtBCD* containing *srtB in trans*, Thr^{131} changed to Arg	Upstream: NlacEF and SrtBT131Rrev; downstream: NlacER and SrtBT131Rfor; fragments from T4Δ*srtBCD*+*lacE*::*srtB* fused by overhang extension PCR	This study
T4Δ*srtABCD*	Erm^R, Kan^R, strain lacking *srtA, srtB, srtC* and *srtD*	SrtA-1/SrtA-4 fragment moved from T4Δ*srtA* to T4Δ*srtBCD*	12; this study
T4Δ*srtABCD*+ *lacE*::*srtB*	Spc^R, Erm^R, Kan^R, quadruple-sortase mutant strain containing *srtB in trans*	SrtA-1/SrtA-4 fragment moved from T4Δ*srtA* to T4Δ*srtBCD*+*lacE*::*srtB*	12; this study
T4Δ*srtABCD*+ *lacE*::*srtC*	Spc^R, Erm^R, Kan^R, quadruple-sortase mutant strain containing *srtC in trans*	SrtA-1/SrtA-4 fragment moved from T4Δ*srtA* to T4Δ*srtBCD*+*lacE*::*srtC*	12; this study
T4Δ*srtABCD*+ *lacE*::*srtD*	Spc^R, Erm^R, Kan^R, quadruple-sortase mutant strain containing *srtD in trans*	SrtA-1/SrtA-4 fragment moved from T4Δ*srtA* to T4Δ*srtBCD*+*lacE*::*srtD*	12; this study

Crystallization, data collection, and processing

Purified SrtC was dialyzed against 50 mM Tris–HCl, 1 mM ethylenediaminetetraacetic acid and concentrated thereafter to 10 mg ml^{-1}. Two different crystallization conditions were established for SrtC. Orthorhombic $P2_12_12_1$ crystals appeared in sitting drop by vapor diffusion in 1.6 M magnesium sulfate and 0.1 M Mes (pH 6.5) at 20 °C (crystal form A) and were also obtained in hanging drops by vapor diffusion in 0.1 M Mes (pH 7.0) and 1.9 M ammonium sulfate at 20 °C (crystal form B). The two crystal structures from SrtC were here termed by their respective PDB codes, 3G66 (crystal form A) and 3G69 (crystal form B). Two microliters of a 10 mg/ml protein solution was mixed in 1 μl of the crystallization reservoir solutions for the hanging drops, and 0.1 μl of the same protein solution in 0.1 μl of the crystallization reservoir solutions for the sitting drops. Both crystal forms were cryoprotected by adding 20% glycerol, followed by flash cooling in liquid nitrogen. Data collection was performed under cryogenic conditions ($T = 100$ K), at beamline ID14-1 in European Synchrotron Radiation Facility (Grenoble, France) ($\lambda = 0.934$ Å) using an ADSC Q210 CCD detector. The diffraction data were processed using MOSFLM.[36] Data collection statistics for the data sets as well as cell dimensions of the two orthorhombic crystals of SrtC are presented in Table 1.

Table 3. Primers used in the study, with restriction enzymes sites

Primer name	Sequence
SrtA-1	aggatgaggacttgattgaagaat
SrtA-2	ttttgggccctatgcttcaccttctgtttcgttt (ApaI site underlined)
SrtA-3	ttttggatcctacaaatcagtgaaatccatgatt (BamHI site underlined)
SrtA-4	tccgataaagtttccgatgaaagt
SrtBT131Rfor	gtgattacggcacatagaggtttgccaacagct
SrtBT131Rrev	agctgttggcaaacctctatgtgccgtaatcac
Dam406	tctatgcctattccagaggaaatggat
Kan-Rev-Apa	ttttgggccctaaaacaattcatccagtaaaat (ApaI site underlined)

Structure determination and refinement

Both crystal structures of SrtC were solved by molecular replacement using the PHASER program.[37] Matthew coefficient calculations suggested the presence of two molecules in the asymmetric units for both crystals.[38] The crystal structures of SrtC were determined using a polyalanine model of SrtB (58% identity and PDB code 2W1J). Successive cycles of manual model building were performed with COOT,[39] with the rigid-body refinement in the initial steps and with the restrained refinement in the later steps by using REFMAC.[40] Five percent of the reflections was set aside for monitoring the refinement by R_{free}.[41] The loop (comprising residues 79–100) was built manually in both crystal structures of SrtC. Besides residues 255–267 at the C-terminal of SrtC, the loop residues 90–97 and 96–98 in chains A and B of SrtC (PDB code 3G66), respectively, could not be modeled due to the poor quality of the electron density. Similarly, we were not able to model the side chains of residues 89–98 and 90–93 in chains A and B of SrtC (PDB code 3G69), respectively. Two 2-(*N*-morpholino)ethanesulfonic acid molecules were added in observed excess densities within both SrtC crystal structures. The final rounds of refinement yielded R_{free} and R_{cryst} values of 23.5% and 18.7% for SrtC (PDB

code 3G66) and 25.8% and 19.2% for SrtC (PDB code 3G69), respectively. The two models conform well to the expected protein geometry and the rmsd of bond lengths from standard values for such resolutions (Table 1). The stereochemistry of the models was analyzed with PROCHECK.[42] Refinement statistics are provided in Table 1. The secondary structure assignment was performed with DSSP.[43] The SSM algorithm was used to calculate rmsd.[44]

Accession numbers

Coordinates and structure factors have been deposited in the Protein Data Bank with accession numbers 3G66 and 3G69.

Acknowledgements

We gratefully acknowledge access to synchrotron radiation at beamline ID14-1 at the European Synchrotron Radiation Facility laboratory, Grenoble, France; at beamline X11 at the DESY laboratory, Hamburg, Germany; at beamline MX-41 at the BESSY laboratory, Berlin, Germany; and at beamline 711 at MAX laboratory, Lund University, Sweden. This study was supported by grants from the Swedish Research Council, the Swedish National Board of Health and Welfare, the Royal Academy of Sciences, Torsten and Ragnar Söderbergs Foundation, the Swedish Foundation for Strategic Research, and the German Research Council. The authors have no conflicting financial interests.

References

1. Cutts, F. T., Zaman, S. M., Enwere, G., Jaffar, S., Levine, O. S., Okoko, J. B. *et al.* (2005). Efficacy of nine-valent pneumococcal conjugate vaccine against pneumonia and invasive pneumococcal disease in The Gambia: randomised, double-blind, placebo-controlled trial. *Lancet*, **365**, 1139–1146.
2. Sandgren, A., Sjostrom, K., Olsson-Liljequist, B., Christensson, B., Samuelsson, A., Kronvall, G. & Henriques Normark, B. (2004). Effect of clonal and serotype-specific properties on the invasive capacity of *Streptococcus pneumoniae*. *J. Infect. Dis.* **189**, 785–796.
3. Barocchi, M. A., Ries, J., Zogaj, X., Hemsley, C., Albiger, B., Kanth, A. *et al.* (2006). A pneumococcal pilus influences virulence and host inflammatory responses. *Proc. Natl. Acad. Sci. USA*, **103**, 2857–2862.
4. Hultgren, S. J., Jones, C. H. & Normark, S. (1996). Bacterial adhesins and their assembly. In *Escherichia coli and Salmonella typhimurium*: *Cellular and Molecular Biology* (Neidhardt, F. C., ed), pp. 2730–2756, American Society for Microbiology Press, Washington, DC.
5. Budzik, J. M., Marraffini, L. A. & Schneewind, O. (2007). Assembly of pili on the surface of Bacillus cereus vegetative cells. *Mol. Microbiol.* **66**, 495–510.
6. Mora, M., Bensi, G., Capo, S., Falugi, F., Zingaretti, C., Manetti, A. G. *et al.* (2005). Group A *Streptococcus* produce pilus-like structures containing protective antigens and Lancefield T antigens. *Proc. Natl Acad. Sci. USA*, **102**, 15641–15646.
7. Nallapareddy, S. R., Singh, K. V., Sillanpaa, J., Garsin, D. A., Hook, M., Erlandsen, S. L. & Murray, B. E. (2006). Endocarditis and biofilm-associated pili of *Enterococcus faecalis*. *J. Clin. Invest.* **116**, 2799–2807.
8. Ton-That, H. & Schneewind, O. (2003). Assembly of pili on the surface of *Corynebacterium diphtheriae*. *Mol. Microbiol.* **50**, 1429–1438.
9. Yanagawa, R. & Honda, E. (1976). Presence of pili in species of human and animal parasites and pathogens of the genus *Corynebacterium*. *Infect. Immun.* **13**, 1293–1295.
10. Butler, J. C., Hofmann, J., Cetron, M. S., Elliott, J. A., Facklam, R. R. & Breiman, R. F. (1996). The continued emergence of drug-resistant *Streptococcus pneumoniae* in the United States: an update from the Centers for Disease Control and Prevention's Pneumococcal Sentinel Surveillance System. *J. Infect. Dis.* **174**, 986–993.
11. Sjostrom, K., Blomberg, C., Fernebro, J., Dagerhamn, J., Morfeldt, E., Barocchi, M. A. *et al.* (2007). Clonal success of piliated penicillin nonsusceptible pneumococci. *Proc. Natl Acad. Sci. USA*, **104**, 12907–12912.
12. Falker, S., Nelson, A. L., Morfeldt, E., Jonas, K., Hultenby, K., Ries, J. *et al.* (2008). Sortase-mediated assembly and surface topology of adhesive pneumococcal pili. *Mol. Microbiol.* **70**, 595–607.
13. Nelson, A. L., Ries, J., Bagnoli, F., Dahlberg, S., Falker, S., Rounioja, S. *et al.* (2007). RrgA is a pilus-associated adhesin in *Streptococcus pneumoniae*. *Mol. Microbiol.* **66**, 329–340.
14. Mazmanian, S. K., Liu, G., Ton-That, H. & Schneewind, O. (1999). *Staphylococcus aureus* sortase, an enzyme that anchors surface proteins to the cell wall. *Science*, **285**, 760–763.
15. Schneewind, O., Model, P. & Fischetti, V. A. (1992). Sorting of protein A to the staphylococcal cell wall. *Cell*, **70**, 267–281.
16. Fischetti, V. A., Pancholi, V. & Schneewind, O. (1990). Conservation of a hexapeptide sequence in the anchor region of surface proteins from Gram-positive cocci. *Mol. Microbiol.* **4**, 1603–1605.
17. Mandlik, A., Swierczynski, A., Das, A. & Ton-That, H. (2008). Pili in Gram-positive bacteria: assembly, involvement in colonization and biofilm development. *Trends Microbiol.* **16**, 33–40.
18. Manzano, C., Contreras-Martel, C., El Mortaji, L., Izore, T., Fenel, D., Vernet, T. *et al.* (2008). Sortase-mediated pilus fiber biogenesis in *Streptococcus pneumoniae*. *Structure*, **16**, 1838–1848.
19. Ton-That, H. & Schneewind, O. (2004). Assembly of pili in Gram-positive bacteria. *Trends Microbiol.* **12**, 228–234.
20. Swaminathan, A., Mandlik, A., Swierczynski, A., Gaspar, A., Das, A. & Ton-That, H. (2007). Housekeeping sortase facilitates the cell wall anchoring of pilus polymers in *Corynebacterium diphtheriae*. *Mol. Microbiol.* **66**, 961–974.
21. LeMieux, J., Woody, S. & Camilli, A. (2008). Roles of the sortases of *Streptococcus pneumoniae* in assembly of the RlrA pilus. *J. Bacteriol.* **190**, 6002–6013.
22. Neiers, F., Madhurantakam, C., Falker, S., Normark, S., Henriques-Normark, B. & Achour, A. (2009). Cloning, expression, purification, crystallization and preliminary X-ray analysis of the pilus-associated sortase C from *Streptococcus pneumoniae*. *Acta Crystallogr., Sect. F: Struct. Biol. Cryst. Commun.* **65**, 55–58.

23. Bond, C. S. (2003). TopDraw: a sketchpad for protein structure topology cartoons. *Bioinformatics*, **19**, 311–312.
24. Ilangovan, U., Ton-That, H., Iwahara, J., Schneewind, O. & Clubb, R. T. (2001). Structure of sortase, the transpeptidase that anchors proteins to the cell wall of *Staphylococcus aureus*. *Proc. Natl Acad. Sci. USA*, **98**, 6056–6061.
25. Maresso, A. W., Wu, R., Kern, J. W., Zhang, R., Janik, D., Missiakas, D. M. *et al.* (2007). Activation of inhibitors by sortase triggers irreversible modification of the active site. *J. Biol. Chem.* **282**, 23129–23139.
26. Zhang, R., Wu, R., Joachimiak, G., Mazmanian, S. K., Missiakas, D. M., Gornicki, P. *et al.* (2004). Structures of sortase B from *Staphylococcus aureus* and Bacillus anthracis reveal catalytic amino acid triad in the active site. *Structure*, **12**, 1147–1156.
27. Zong, Y., Bice, T. W., Ton-That, H., Schneewind, O. & Narayana, S. V. (2004). Crystal structures of *Staphylococcus aureus* sortase A and its substrate complex. *J. Biol. Chem.* **279**, 31383–31389.
28. Zong, Y., Mazmanian, S. K., Schneewind, O. & Narayana, S. V. (2004). The structure of sortase B, a cysteine transpeptidase that tethers surface protein to the *Staphylococcus aureus* cell wall. *Structure*, **12**, 105–112.
29. Folch, B., Rooman, M. & Dehouck, Y. (2008). Thermostability of salt bridges *versus* hydrophobic interactions in proteins probed by statistical potentials. *J. Chem. Inf. Model.* **48**, 119–127.
30. Reid, K. C., Lindley, P. F. & Thornton, J. M. (1985). Sulphur-aromatic interactions in proteins. *FEBS Lett.* **190**, 209–2013.
31. Viguera, A. R. & Serrano, L. (1995). Side-chain interactions between sulfur-containing amino acids and phenylalanine in α-helices. *Biochemistry*, **34**, 8771–8779.
32. Ton-That, H., Liu, G., Mazmanian, S. K., Faull, K. F. & Schneewind, O. (1999). Purification and characterization of sortase, the transpeptidase that cleaves surface proteins of *Staphylococcus aureus* at the LPXTG motif. *Proc. Natl Acad. Sci. USA*, **96**, 12424–12429.
33. Matagne, A., Dubus, A., Galleni, M. & Frere, J. M. (1999). The β-lactamase cycle: a tale of selective pressure and bacterial ingenuity. *Nat. Prod. Rep.* **16**, 1–19.
34. Sung, C. K., Li, H., Claverys, J. P. & Morrison, D. A. (2001). An rpsL cassette, janus, for gene replacement through negative selection in *Streptococcus pneumoniae*. *Appl. Environ. Microbiol.* **67**, 5190–5196.
35. Lau, P. C., Sung, C. K., Lee, J. H., Morrison, D. A. & Cvitkovitch, D. G. (2002). PCR ligation mutagenesis in transformable streptococci: application and efficiency. *J. Microbiol. Methods*, **49**, 193–205.
36. Leslie, A. G. (2006). The integration of macromolecular diffraction data. *Acta Crystallogr., Sect. D: Biol. Crystallogr.* **62**, 48–57.
37. McCoy, A. J. (2007). Solving structures of protein complexes by molecular replacement with Phaser. *Acta Crystallogr., Sect. D: Biol. Crystallogr.* **63**, 32–41.
38. Matthews, B. W. (1968). Solvent content of protein crystals. *J. Mol. Biol.* **33**, 491–497.
39. Emsley, P. & Cowtan, K. (2004). Coot: model-building tools for molecular graphics. *Acta Crystallogr., Sect. D: Biol. Crystallogr.* **60**, 2126–2132.
40. Vagin, A. A., Steiner, R. A., Lebedev, A. A., Potterton, L., McNicholas, S., Long, F. & Murshudov, G. N. (2004). REFMAC5 dictionary: organization of prior chemical knowledge and guidelines for its use. *Acta Crystallogr., Sect. D: Biol. Crystallogr.* **60**, 2184–2195.
41. Brunger, A. T. (1992). Free R value: a novel statistical quantity for assessing the accuracy of crystal structures. *Nature*, **355**, 472–475.
42. Laskowski, R. A., Moss, D. S. & Thornton, J. M. (1993). Main-chain bond lengths and bond angles in protein structures. *J. Mol. Biol.* **231**, 1049–1067.
43. Kabsch, W. & Sander, C. (1983). Dictionary of protein secondary structure: pattern recognition of hydrogen-bonded and geometrical features. *Biopolymers*, **22**, 2577–2637.
44. Krissinel, E. & Henrick, K. (2004). Secondary-structure matching (SSM), a new tool for fast protein structure alignment in three dimensions. *Acta Crystallogr., Sect. D: Biol. Crystallogr.* **60**, 2256–2268.